

An observational link between AGN Eddington ratio and [N II] λ 6583/H α at $0.6 < z < 1.7$

KYUSEOK OH,^{1,*} YOSHIHIRO UEDA,¹ MASAYUKI AKIYAMA,² HYEWON SUH,^{3,†} MICHAEL J. KOSS,⁴ DAICHI KASHINO,⁵ AND GÜNTHER HASINGER⁶

¹*Department of Astronomy, Kyoto University, Kitashirakawa-Oiwake-cho, Sakyo-ku, Kyoto 606-8502, Japan*

²*Astronomical Institute, Tohoku University, Aramaki, Aoba-ku, Sendai, Miyagi 980-8578, Japan*

³*Subaru Telescope, National Astronomical Observatory of Japan (NAOJ), National Institutes of Natural Sciences (NINS), 650 North A'ohoku place, Hilo, HI 96720, USA*

⁴*Eureka Scientific, 2452 Delmer Street Suite 100, Oakland, CA 94602-3017, USA*

⁵*Department of Physics, ETH Zürich, Wolfgang-Pauli-Strasse 27, CH-8093, Zürich, Switzerland*

⁶*European Space Astronomy Centre (ESA/ESAC), Director of Science, E-28691 Villanueva de la Cañada, Madrid, Spain*

(Received March 29, 2019; Revised May 29, 2019; Accepted June 8, 2019)

ABSTRACT

We present an observed relationship between Eddington ratio (λ_{Edd}) and optical narrow-emission-line ratio ([N II] λ 6583/H α) of X-ray-selected broad-line active galactic nuclei (AGN) at $0.6 < z < 1.7$. We use 27 near-infrared spectra from the Fiber Multi-Object Spectrograph along with 26 sources from the literature. We show that the λ_{Edd} and [N II] λ 6583/H α ratio at $0.6 < z < 1.7$ exhibits a similar anti-correlation distribution of $\lambda_{\text{Edd}} - [\text{N II}]\lambda 6583/\text{H}\alpha$ as has been found for local ($\langle z \rangle = 0.036$), ultra-hard X-ray selected AGN. The observed distribution implies that there is a consistent relationship from local to $z \sim 1.7$ which corresponds from the present time to 4 Gyr old. Further study of high redshift low Eddington ratio AGN ($\log \lambda_{\text{Edd}} < -2$) is necessary to determine fully whether the $\lambda_{\text{Edd}} - [\text{N II}]\lambda 6583/\text{H}\alpha$ anti-correlation still holds in high-redshift AGN at low Eddington ratios.

Keywords: galaxies: active — galaxies: Seyfert — galaxies: nuclei — quasars: general

1. INTRODUCTION

Nebular emission lines play an important role in modern astronomy. Forbidden emission lines (e.g., [O III] λ 5007, [N II] λ 6584, and [S II] λ 6717, 6731) and Balmer lines (H α , H β) in the optical band are frequently used to diagnose the physical state of active galactic nuclei (AGN) and star-forming activity (Baldwin et al. 1981; Veilleux & Osterbrock 1987; Kewley et al. 2001; Schawinski et al. 2007) and applied to distinguish central nuclear activity from star-formation. In AGN, higher ratios of collisionally excited forbidden lines are predicted because AGN produce more high energy photons than star-forming regions in a galaxy, which produce photoionization-induced Balmer emission lines. Both forbidden lines and Balmer lines are easy to detect as they are prominent in AGN hosts

and star-forming galaxies. Due to being closely located in wavelength these lines suffer similar extinction and their ratios can therefore be used independent of extinction. In the framework of AGN unified model (Antonucci 1993; Urry & Padovani 1995), furthermore, these prominent narrow emission-lines are extended on kpc scales and thus are visible regardless of accretion rate and viewing angle. Despite its efficiency as a useful diagnostic tool, several studies have reported that heavily obscured or dusty AGN and those with significant star formation may not be diagnosed as AGN using emission-line spectroscopy since obscuration and star formation can dilute emission-line strengths originated from AGN (Elvis et al. 1981; Iwasawa et al. 1993; Griffiths et al. 1995; Barger et al. 2001; Comastri et al. 2002; Rigby et al. 2006; Caccianiga et al. 2007; Trump et al. 2015; Koss et al. 2017).

Massive spectroscopic surveys such as Sloan Digital Sky Survey (York et al. 2000) have made it possible to explore emission-line properties, diagnostics, and Eddington ratios (λ_{Edd}) of sizeable sample of local AGN. For example, Kewley et al. (2006) showed

Corresponding author: Kyuseok Oh
ohk@kusastro.kyoto-u.ac.jp

* JSPS Fellow

† Subaru Fellow

that 85224 local emission-line galaxies selected from the SDSS at $0.04 < z < 0.10$ have a positive correlation between λ_{Edd} and a distance from the LINER regime in the $[\text{O III}]\lambda 5007/\text{H}\beta$ versus $[\text{O I}]\lambda 6300/\text{H}\alpha$ diagram (see Fig.19 in Kewley et al. 2006). Later, Stern & Laor (2013) presented emission-line diagnostics of 3175 nearby broad-line AGN from the SDSS ($z < 0.31$) and found a dependence on λ_{Edd} .

Over the last decade new facilities in high-energy astrophysics such as *INTEGRAL* (Winkler et al. 2003), *Swift* (Gehrels et al. 2004), and *NuSTAR* (Harrison et al. 2013) and their observations of AGN have greatly helped to explore the nature of obscured AGN even including Compton-thick sources (e.g., Ricci et al. 2015; Marchesi et al. 2018). High energy photons (> 10 keV) are only biased against Compton-thick levels of obscuration at $\log N_{\text{H}} > 24.5 \text{ cm}^{-2}$ and are not subject to host galaxy contamination or dust obscuration (Koss et al. 2016). Since 2004 December, in particular, the Burst Alert Telescope (BAT, Barthelmy et al. 2005) on the *Swift* satellite (Gehrels et al. 2004) has been successfully carrying all-sky hard X-ray observation (14 – 195 keV), providing monthly lightcurves as well as X-ray spectra (Markwardt et al. 2005; Tueller et al. 2008, 2010; Baumgartner et al. 2013; Oh et al. 2018). The most recent publication of *Swift*-BAT all-sky hard X-ray survey¹ reached a sensitivity of $8.40 \times 10^{-12} \text{ erg cm}^{-2} \text{ s}^{-1}$ over 90% of the sky, identifying 1632 X-ray sources, of which 1099 are AGN including beamed sources (Oh et al. 2018).

Over the past 5 years a massive effort has been made in investigating complete census of black hole masses (M_{BH}) and accretion rates normalized by M_{BH} (λ_{Edd} , $\lambda_{\text{Edd}} \equiv L_{\text{bol}}/L_{\text{Edd}}$, where $L_{\text{Edd}} \equiv 1.3 \times 10^{38} (M_{\text{BH}}/M_{\odot})$) of X-ray selected AGN. Based on the 70-month catalog of *Swift*-BAT (Baumgartner et al. 2013), which identified 836 AGN, the BAT AGN Spectroscopic Survey Data Release 1 (BASS-DR1², Koss et al. 2017; Lamperti et al. 2017; Ricci et al. 2017) published M_{BH} , λ_{Edd} , narrow/broad emission-line strength, emission-line diagnostics, stellar velocity dispersion, and X-ray spectral properties for 642 AGN ($\langle z \rangle \sim 0.05$) using various public surveys (the Sloan Digital Sky Survey and the 6dF Galaxy Survey; Abazajian et al. 2009; Jones et al. 2009; Alam et al. 2015) and dedicated follow-up optical/near-infrared spectroscopic observations.

Using optical emission-line strengths, bolometric luminosity (L_{bol}), and M_{BH} for ~ 300 local AGN ($\langle z \rangle \sim 0.036$, Fig 1), Oh et al. (2017) showed that the $[\text{N II}]\lambda 6583/\text{H}\alpha$ ratio exhibits a significant anti-correlation with λ_{Edd} ($R_{\text{Pear}} = -0.44$, p -value = 3×10^{-13} , root-mean-square deviation $\sigma = 0.28$ dex). The authors confirmed that the reported anti-correlation still holds good in both broad-line and narrow-line AGN, and it is free from different apertures affects that applied for the heterogeneous observations in the BASS-DR1. With a measured anti-correlation with 0.28 dex of σ the $[\text{N II}]\lambda 6583/\text{H}\alpha$ ratio could, in principle, be used to infer accretion efficiencies of high-redshift obscured AGN.

At high redshifts, X-ray observations provide the most complete and numerous samples of AGN including obscured, unobscured, and lower luminosity AGN. For instance, the deepest *Chandra* surveys can reach AGN that are 100 times less luminous than wide field optical surveys where AGN are 500 times more numerous (Brandt & Alexander 2010). While the X-rays provide a reliable tracer of bolometric luminosity up to Compton-thick levels, the black hole mass and Eddington ratio require further observations. For distant obscured AGN, the bulge velocity dispersion, which can be turned into M_{BH} and eventually λ_{Edd} assuming $M_{\text{BH}} - \sigma_*$ relation holds at high redshift, is extremely challenging to measure at high S/N to estimate a black hole mass due to the faintness of the host galaxy.

In this paper, we investigate the observed relationship between λ_{Edd} and the narrow-emission-line ratio, $[\text{N II}]\lambda 6583/\text{H}\alpha$, using 53 X-ray selected broad-line AGN at $0.6 < z < 1.7$, extending the previous study of Oh et al. (2017) beyond the local Universe. This paper is organized as follows. In Section 2, we describe the samples we collated from the literature, and present the spectral line fitting results. In Section 3, we show the observed relationship between λ_{Edd} and $[\text{N II}]\lambda 6583/\text{H}\alpha$ ratio at $0.6 < z < 1.7$. Finally, we discuss our findings and summarize our result in Section 4, with caveats and cautions. We assume a cosmology with $h = 0.70$, $\Omega_{\text{M}} = 0.30$, and $\Omega_{\Lambda} = 0.70$ throughout this work.

2. SAMPLE SELECTION, DATA, AND MEASUREMENTS

In order to investigate the observed link between λ_{Edd} and $[\text{N II}]\lambda 6583/\text{H}\alpha$ at higher redshifts ($\langle z \rangle \sim 1.3$) to directly compare it with the previous study using ultra-hard X-ray selected AGN in the local Universe ($\langle z \rangle \sim 0.036$, Oh et al. 2017), we constructed our samples from literature as follows:

1. Unobscured AGN that have spectroscopically confirmed redshifts featuring broad-emission-lines.

¹ <http://heasarc.gsfc.nasa.gov/docs/swift/results/bs105mon/>

² <http://bass-survey.com>

Table 1. Summary of Samples

Literature / Survey ^a	N ^b	Inst. L_{bol} ^c	Inst. M_{BH} ^d	Inst. $[\text{N II}] \lambda 6583/\text{H}\alpha$ ^e
Harrison et al. 2016 / KASHz	7	<i>XMM-Newton</i> , CDF-S	VLT/KMOS	VLT/KMOS
Merloni et al. 2010; Kartaltepe et al. 2015 / FMOS-COSMOS	2	CCLS	VLT/VIMOS	Subaru/FMOS
Matsuoka et al. 2013; Kartaltepe et al. 2015 / FMOS-COSMOS	17	CCLS	Subaru/FMOS	Subaru/FMOS
Nobuta et al. 2012 / SXDS	9	<i>XMM-Newton</i>	Subaru/FMOS	Subaru/FMOS
Suh et al. 2015 / FMOS-COSMOS	11	CDF-S, <i>XMM-LH</i>	Subaru/FMOS	Subaru/FMOS
Suh et al. (<i>in prep.</i>) / FMOS-COSMOS	7	CCLS	Subaru/FMOS	Subaru/FMOS

^aSource of literature with name of the survey.

^bSize of sample.

^cTelescope or survey used to measure 2-10 keV luminosity.

^dTelescope/instrument used to measure M_{BH} .

^eTelescope/instrument used to measure [N II] λ 6583/H α narrow-emission-line ratio.

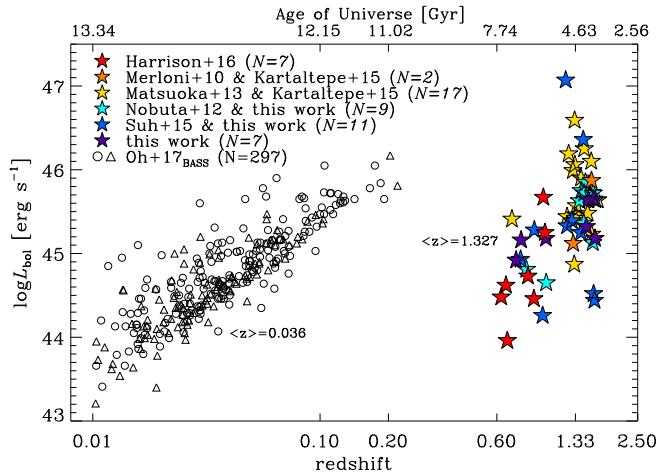


Figure 1. Bolometric luminosity as a function of redshift. Empty circles (broad-line AGN) and triangles (narrow-line AGN) in black are local hard X-ray selected AGN from the BASS-DR1 (Koss et al. 2017; Oh et al. 2017). The high-redshift ($z \sim 1.3$) X-ray-selected broad-line AGN used in this work are shown with color-filled stars.

2. X-ray selected AGN whose intrinsic rest-frame 2-10 keV luminosities are available.
3. Those with deblended narrow-emission-line profiles in [N II] λ 6584 and H α .

We briefly describe the literature used in our investigation in the following section.

2.1. The Subaru / XMM-Newton Deep Survey

The Subaru / XMM-Newton Deep Survey (SXDS) (Sekiguchi et al. 2005) is one of the largest, multiwavelength survey that combines dedicated spectroscopic observations from the far-UV to mid-IR (Nobuta et al.

2012; Akiyama et al. 2015) with soft (0.5 – 2 keV) and hard (2 – 10 keV) band X-ray observations (Ueda et al. 2008). The SXDS field (R.A.: 02^h18^m, decl.: –05°) was observed with XMM-Newton using 100 ks of exposure for a central 30' diameter field and 50 ks for 6 flanking fields. Out of 896 broad-line AGN candidates observed in the SXDS survey, 851 sources were observed using the Fiber Multi-Object Spectrograph (FMOS) on the Subaru telescope (Kimura et al. 2010). The FMOS was used to observe the wavelength between 9000Å and 18000Å with a spectral resolution of $R \sim 800$ at $\lambda \sim 1.55\mu\text{m}$ in the low-resolution mode. Due to the faintness of the targets, 586 optical and near-infrared spectra of the total 896 sources were observed (Nobuta et al. 2012).

In this work, we performed spectral line fitting for 84 sources out of these 586, whose broad H α components as well as [N II] λ 6584 and narrow H α lines are measurable at $0.63 < z < 1.70$. We used *gandalf* IDL code (Sarzi et al. 2006), which was originally developed for spectral line decomposition of the 72 early-type galaxies of full SAURON sample (Bacon et al. 2001) and was applied later to more than 660,000 nearby SDSS narrow emission-line galaxies (Oh et al. 2011)³. Following the application of *gandalf* procedures in Oh et al. (2015), we first deredshifted FMOS spectra taking into account Galactic foreground extinction (Schlafly & Finkbeiner 2011). We then fitted the wavelength region of interest (6000Å–6750Å) focusing on deblending [N II] λ 6584 and narrow H α emission-lines along with broad H α component using Gaussian emission-line templates. The [N II] λ 6548 and [N II] λ 6584 lines were tied each other

³ <http://gem.yonsei.ac.kr/ossy/>

with a pair of Gaussians holding the theoretical ratio of 2.96. Gaussian line widths were set as free parameters with upper limits of 600 km s^{-1} for the narrow-lines and $10,000 \text{ km s}^{-1}$ for the broad lines, respectively. When necessary, multiple Gaussian components were applied to fit broad $\text{H}\alpha$ components following established procedures (Collin et al. 2006; La Mura et al. 2007; Mullaney & Ward 2008). After fitting, 9 reliable fits showing deblended $[\text{N II}]\lambda 6584$ and $\text{H}\alpha$ narrow emission-lines along with a broad $\text{H}\alpha$ component (Fig. 5) were found. The majority of the remaining sources show low signal-to-noise ratio or dominant broad $\text{H}\alpha$ emission features with indistinguishable narrow emission-lines.

Black hole mass measurements relying on single-epoch spectra are commonly used for broad-line AGN (Kaspi et al. 2000; McLure & Dunlop 2002; Vestergaard 2002; Woo & Urry 2002; Greene & Ho 2005; Shen et al. 2008; Vestergaard & Osmer 2009; Shen & Liu 2012; Trakhtenbrot & Netzer 2012; Matsuoka et al. 2013). Virial black hole mass estimation assumes that gravity of a central black hole governs the kinematics of broad-line region (BLR), which yields the relationship between black hole mass, gas velocity, and radius of the BLR ($M_{\text{BH}} \propto R\Delta V^2/G$). Broad Balmer lines (typically $\text{H}\beta$ and $\text{H}\alpha$) are used as a proxy of the average gas velocity, and the $R_{\text{BLR}} - L$ relation obtained through reverberation mapping technique (Kaspi et al. 2000, 2005; Bentz et al. 2006, 2013) provides the radius of the BLR. We estimated the black hole mass of broad-line AGN using the broad $\text{H}\alpha$ luminosity and line width following Greene & Ho (2005).

We estimated the bolometric luminosities of broad-line AGN using the intrinsic $2 - 10 \text{ keV}$ rest-frame luminosity provided by Nobuta et al. (2012) and the median bolometric correction ($k = 20$) as measured by Vasudevan et al. (2009). We applied the same bolometric correction to the same energy band ($2 - 10 \text{ keV}$) following that of Oh et al. (2017). We calculated λ_{Edd} ($L_{\text{Edd}} \equiv L_{\text{bol}}/L_{\text{Edd}}$) by combining the estimated L_{bol} and L_{Edd} , assuming $L_{\text{Edd}} \equiv 1.3 \times 10^{38} (M_{\text{BH}}/M_{\odot})$. A summary of the samples is provided in Tab. 1 with measured quantities provided in Tab. 2.

2.2. The FMOS / X-ray surveys

The *Chandra* COSMOS Legacy Survey (CCLS, Civano et al. 2016) is a 2.2 deg^2 *Chandra* survey of the COSMOS field with a total exposure time of 4.6 Ms. The CCLS point source catalog provides X-ray measurements for 4016 X-ray point sources and their $2 - 10 \text{ keV}$ fluxes. Spectroscopic follow-up observations of the CCLS field have been carried in optical with DEIMOS (Hasinger et al. 2018) and in NIR with

FMOS (Silverman et al. 2015; Kashino et al. 2019, Suh et al. in prep.). In this field, we employ three samples using NIR spectroscopy with FMOS.

The first used the low-resolution mode of FMOS, which covers from 9000\AA to 18000\AA with a dispersion of $\sim 5\text{\AA} \text{ pixel}^{-1}$. Kartaltepe et al. (2015) obtained 119 near-infrared spectroscopic data including $[\text{N II}]\lambda 6583/\text{H}\alpha$ emission-line ratio selected from the COSMOS field at $z < 1.7$. Matsuoka et al. (2013) also obtained 43 near-infrared spectra of moderate-luminosity broad-line AGN at $z < 1.8$ found in the COSMOS and Extended Chandra Deep Field-South Survey, using the low-resolution mode of FMOS instrument. Another effort on measuring M_{BH} of 89 broad-line AGN in the COSMOS field at $1 < z < 2.2$ had been made by Merloni et al. (2010) using the VIMOS multi-object spectrograph on the European Southern Observatory’s Very Large Telescope (ESO-VLT) and virial black hole masses derived from MgII line width and continuum luminosity (L_{3000}) (McGill et al. 2008) were made. Although these archival spectra provide at least several dozen high redshift unobscured AGN samples with key quantities such as M_{BH} measured from the broad-line (either $\text{H}\alpha$ or MgII) and bolometric luminosity from the $2 - 10 \text{ keV}$ flux, however, the total number of usable sources in such a redshift range ($z < \sim 2$) is limited due to the availability of the $[\text{N II}]\lambda 6584$ and $\text{H}\alpha$ line ratio ($N = 19$).

In addition to these 19 sources, we obtained 18 sources from the X-ray selected broad-line AGN sample of FMOS-COSMOS survey (Schulze et al. 2018, Suh et al. in prep.), at redshifts $0.73 < z < 1.63$. The FMOS high-resolution mode observations cover four spectral regions (J-short: $0.92 - 1.12\mu\text{m}$, J-long: $1.11 - 1.35\mu\text{m}$, H-short: $1.40 - 1.60\mu\text{m}$, H-long: $1.60 - 1.80\mu\text{m}$) with a spectral resolution of $R \sim 2600$. More details of the survey design, instrumental performance, and observations, can be found in Silverman et al. (2015).

The bolometric luminosity and Eddington ratio of these sources were estimated using available X-ray catalogues such as CCLS (Civano et al. 2016), *Chandra* Deep Field South (CDF-S) (Xue et al. 2011), Extended *Chandra* Deep Field South (E-CDF-S) (Lehmer et al. 2005), and *XMM-Newton*-Lockman Hole (*XMM*-LH) (Brunner et al. 2008). In order to estimate bolometric luminosity (L_{bol}), we applied a bolometric correction ($k = 20$) to an absorption-corrected rest-frame $2 - 10 \text{ keV}$ luminosity.

We disentangled the broad $\text{H}\alpha$ and narrow-lines for 18 sources from the FMOS-COSMOS survey (Silverman et al. 2015, Suh et al. in prep.) by applying the spectral line fitting as same as that of the SXDS

data shown in the Section 2.1. The achieved spectral line fit for the 18 sources are shown in Fig. 6 and Fig. 7. By adopting single-epoch virial mass estimation recipe of Greene & Ho (2005, equation 9), we computed the M_{BH} from the broad H α line widths and luminosities.

2.3. KASHz AGN survey

The KMOS (*K*-band Multi-Object Spectrograph) AGN Survey at High redshift (KASHz) provides measurements of the broad H α , narrow H α , and [N II] λ 6584 emission lines as well as 2 – 10 keV measurements for 7 broad-line AGN at $0.63 < z < 0.98$ (Harrison et al. 2016). The authors compiled the X-ray measurements for those 7 broad-line AGN from the 4 Ms CDFS catalogue (Xue et al. 2011) and 400 ks SXDS catalog (Ueda et al. 2008).

3. [N II] λ 6583/H α AND EDDINGTON RATIO RELATION AT $0.6 < Z < 1.7$

We show the distribution of narrow [N II] λ 6583/H α as a function of λ_{Edd} for the 53 X-ray selected broad-line AGN at $0.6 < z < 1.7$ in Fig. 2. Local hard X-ray selected AGN at $\langle z \rangle \sim 0.036$ (Oh et al. 2017) are also shown with the filled contours along with the measured Bayesian linear regression fit (thin dashed line, equation 1). Using 297 local AGN, Oh et al. (2017) reported the statistically significant anti-correlation with $(-1.48 \pm 0.04, -0.98 \pm 0.13)$ of (α, β) , -0.44 of the Pearson R coefficient, 3×10^{-13} of p -value, and 0.28 dex of the root-mean-square (rms) deviation.

$$\log([\text{N II}] \lambda 6583/\text{H}\alpha) = \alpha + \beta \log \lambda_{\text{Edd}} \quad (1)$$

We find that the distribution of [N II] λ 6583/H α as a function of λ_{Edd} at $0.6 < z < 1.7$ is approximately similar with that of local AGN, mainly occupying high λ_{Edd} regime with -0.86 of median $\log \lambda_{\text{Edd}}$. Unlike local AGN, statistical significance of the linear regression analysis for these high- z AGN is too poor to draw any definite relation at this time ($R_{\text{Pear}} = -0.14$, p -value = 0.54) because of a lack of low Eddington ratio sources.

Confirming that the [N II] λ 6583/H α vs. λ_{Edd} relation still holds true for high- z AGN, as is hinted in Fig. 2, requires a much larger number of low λ_{Edd} AGN at $\log \lambda_{\text{Edd}} < -2$. Indeed, Suh et al. (2015) reported that broad-line AGN at $1 < z < 2.2$ showing $\log \lambda_{\text{Edd}} < -2$ are very rare from their Subaru/FMOS observation for X-ray selected AGN along with previously published literature (Gavignaud et al. 2008; Merloni et al. 2010; Shen et al. 2011; Nobuta et al. 2012; Matsuoka et al. 2013), as seen in Fig 2. Therefore, future high-resolution

near-infrared spectroscopic observations for a statistically sizeable sample of low λ_{Edd} AGN at $\log \lambda_{\text{Edd}} < -2$ are required to confirm the correlation.

We perform the Kolmogorov-Smirnov test (K–S test) for [N II] λ 6583/H α using sub-sample of local and high- z AGN based on the same range of $\log \lambda_{\text{Edd}}$ (> -1.81). We find that [N II] λ 6583/H α distribution of local and high- z AGN are consistent with being drawn from the same underlying probability distribution with 0.11 of D statistic and 0.66 of p -value. We therefore find that while we cannot find a statistically significant linear correlation within the current dataset, the overall distribution of values is consistent with those at low redshifts.

Our sample of unobscured (broad-line) AGN covers the black hole mass range $6.9 < \log(M_{\text{BH}}/M_{\odot}) < 9.3$ and the bolometric luminosity range $44.0 < \log L_{\text{bol}} < 47.1$ with the Eddington ratio ranging from -2.29 to -0.07 (Fig. 3). Compared to the local AGN shown in Fig. 3, the M_{BH} distribution of high- z AGN is not particularly different (0.11 of p -value from the K–S test) while the L_{bol} (3.1×10^{-11} of p -value) and their resultant derivative, λ_{Edd} (3.8×10^{-6} of p -value), are generally higher than those of local AGN. Using 929 X-ray selected AGN at $\langle z \rangle \sim 1.5$, Lusso et al. (2012) showed that both types of AGN have higher Eddington ratio at higher redshift at any given M_{BH} , which is in agreement with Netzer & Trakhtenbrot (2007) who used a sample of 9818 SDSS broad-line AGN at $z \leq 0.75$. It should be noted that these literature adopted a different bolometric correction factors, spectral line fitting techniques estimating black hole mass (i.e., L_{Edd}) from a different wavelength regime and redshift. Nevertheless, the observed trend of λ_{Edd} shown in Fig. 3 is generally consistent with the literature.

4. DISCUSSION

In this section, we introduce caveat that should be taken into account when interpreting results, such as inconclusive correlation in the linear regression and selection bias. Then, we discuss role of mass-metallicity relation in the current sample. We also present positive correlations between N V λ 1240 involved emission-line ratios and λ_{Edd} stating interpretations that help to understand observations. Lastly, we state lack of metallicity evolution of AGN with redshift.

The current samples used in this investigation are not enough to define the relation between λ_{Edd} and [N II] λ 6583/H α at high-redshift. As it is described in the Section 3, our sample of 53 AGN is neither complete nor fully representative of the high-redshift AGN. Nevertheless, we provide an observational hint that AGN beyond

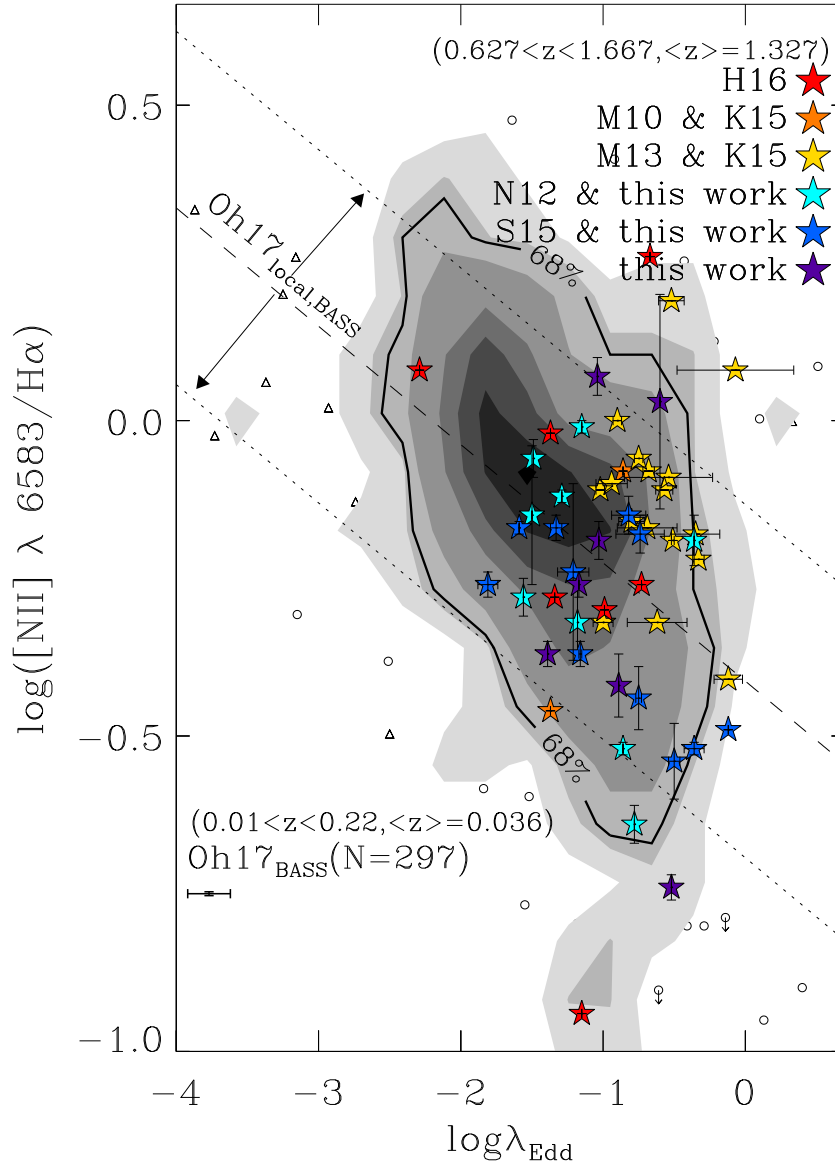


Figure 2. $[\text{N II}]\lambda 6583/\text{H}\alpha$ versus λ_{Edd} diagram for local and high- z X-ray selected broad-line AGN. The $[\text{N II}]\lambda 6583/\text{H}\alpha$ vs. λ_{Edd} relationship for local ($\langle z \rangle \sim 0.036$) hard X-ray selected AGN from Oh et al. (2017) is shown with dashed-line, along with the rms deviation (0.28 dex, dotted-lines) and filled contours. The Pearson correlation coefficient and p -value are -0.44 and 3×10^{-13} , respectively. X-ray selected broad-line AGN at $0.626 < z < 1.667$ are presented with color-filled stars. When available, the measurements errors in both abscissa and ordinate are presented.

local Universe up to $z \sim 1.7$ follow the same trend in λ_{Edd} and $[\text{N II}]\lambda 6583/\text{H}\alpha$ as low redshift AGN.

4.1. Selection bias

A possible selection bias could be present in our sample. The observability of the broad $\text{H}\alpha$ emission-line and narrow lines ($[\text{N II}]\lambda 6584$ and $\text{H}\alpha$) and following spectral line fitting are highly dependent on the line strengths and noise level of the spectra (i.e., S/N). Observational limitations caused by sensitivity of the instruments in

such a high-redshift sample could lead us only to detect sources with prominent narrow emission-lines compared to the broad lines. Similarly, this is also true for L_{bol} that estimated from the X-ray surveys, which is not free from the survey flux limit. It should be noted that the primary flux limit is based on the ability to measure narrow emission-lines and lower Eddington ratio sources need much more sensitive observations in the NIR. Fig. 3 and Fig. 4 present distribution of bolometric luminosity and Eddington ratio for local and high- z

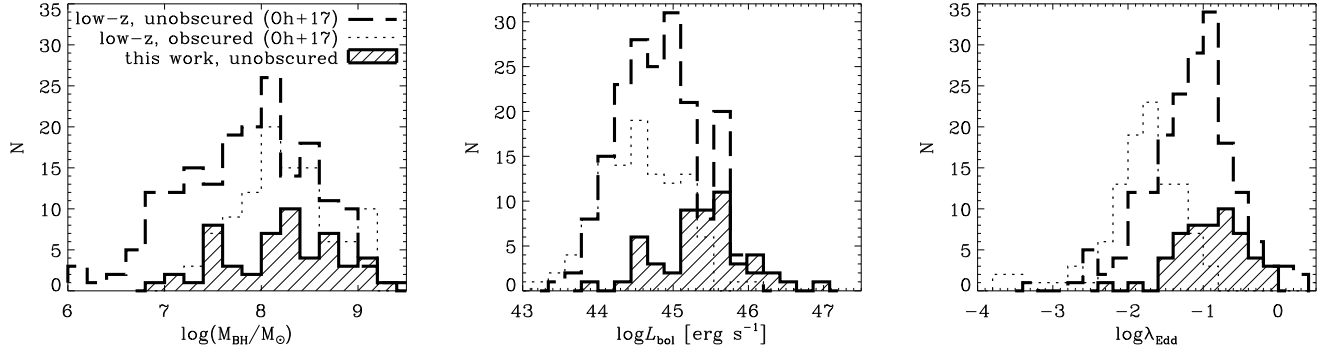


Figure 3. Histograms of $\log(M_{\text{BH}}/M_{\odot})$ (left-hand panel), $\log L_{\text{bol}}$ (middle), and $\log \lambda_{\text{Edd}}$ (right) for high- z AGN (hatched area), local obscured (narrow-line) AGN (dotted lines), and local unobscured (broad-line) AGN (long-dashed lines).

AGN. It is clearly seen that the high- z AGN presented in this work appear to be clumping in high L_{bol} and λ_{Edd} .

The distribution of the [N II] λ 6583/H α ratio reported in this paper and that of Oh et al. (2017) is similar to that of the 12 μm local AGN sample (Malkan et al. 2017). The 12 μm sample is representative of the local AGN population as it covers nearly six orders of magnitude in luminosity and because it is relatively unaffected by obscuration. Malkan et al. (2017) investigated the optical and ultraviolet spectroscopic properties of 81 broad-line AGN and 104 narrow-line AGN and found the $\log([\text{N II}]\lambda 6583/\text{H}\alpha)$ ratio distribution has a median value of -0.14 compared to -0.19 (this work) and -0.15 (Oh et al. 2017). The [N II] λ 6583/H α distribution of the IRAS 12 μm AGN shows a somewhat broader distribution, compared to the X-ray selected local AGN and those in the present work, with a tail to low values of [N II] λ 6583/H α . The similar distributions of the [N II] λ 6583/H α ratio in X-ray and IR selected AGN imply that $\lambda_{\text{Edd}} - [\text{N II}]\lambda 6583/\text{H}\alpha$ relationship is probably not only confined to X-ray selected sample.

4.2. Physical interpretations

In Oh et al. (2017) we discussed various complications such as the uncertainty in bolometric correction and AGN variability as a source of inherent scatter. We also discussed effect of mass-metallicity ($M_* - Z$) relation, X-ray heating, radiative-driven wind as possible mechanisms explaining the relationship between AGN Eddington ratio (λ_{Edd}) and [N II] λ 6583/H α ratio (see Oh et al. 2017 for discussions and references therein).

Larson (1974) predicted that metal abundances in galaxies depend on their stellar mass, as small galaxies experience large amount of gas loss via galactic winds. This picture was later observationally supported by Garnett (2002) and Tremonti et al. (2004). Narrow emission-line ratios in AGN have been reported to have a correlation with stellar mass as in

star-forming galaxies (Groves et al. 2006; Stern & Laor 2013). The same trend is also known for broad-line AGN (Hamann & Ferland 1999). A positive relation between emission-line ratios and M_{BH} has been reported (Shemmer & Netzer 2002; Warner et al. 2004; Nagao et al. 2006a,b; Matsuoka et al. 2009, 2011; Oh et al. 2017). As it has been reported by Oh et al. (2017), however, not all emission-line ratios show statistically significant dependences on M_{BH} and λ_{Edd} . If emission-line ratios and λ_{Edd} are tightly related due to $M_* - Z$ relation, other metallicity-sensitive emission-line ratios also should have shown the similar dependency. This implies that there are other important factors on the relationship between the emission-line ratios and λ_{Edd} .

It should be noted that Matsuoka et al. (2011) reported positive correlations between N V λ 1240 involved emission-line ratios and λ_{Edd} using composite spectra of the SDSS quasars at $2.3 < z < 3.0$. Considering the fact that N V λ 1240 broad emission-line is originated from regions much closer to the supermassive black hole in a sub-parsec scale, it is natural to depict N V λ 1240 and [N II] λ 6584 behave independently. As Matsuoka et al. (2011) pointed out, composite spectra of luminous SDSS quasars seem to be associated with a post-starburst phase near the circumnuclear region that enriching nitrogen abundance by AGB stars, which is a different physical mechanism than that of the AGN samples explored in this work. Furthermore, distributions of L_{bol} , M_{BH} , and λ_{Edd} for the 2678 SDSS quasars used in their work show that these quasars exhibit more than an order of magnitude larger L_{bol} , M_{BH} , and λ_{Edd} than those presented in this work. As their samples are observed in higher redshift with intermediate spectral resolution ($R \sim 2000$) optical spectrograph, bright quasars are preferentially selected, which in turn showing remarkably luminous, massive and high Eddington ratio quasars. As a result, baseline of λ_{Edd} is partially restricted from -1.1

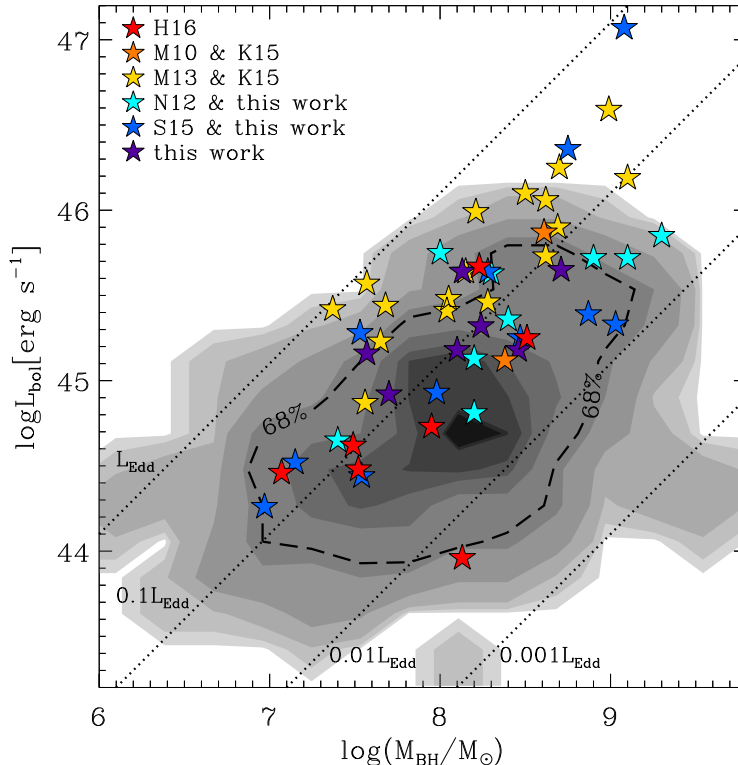


Figure 4. Bolometric luminosity vs. black hole mass for local ($\langle z \rangle \sim 0.036$, achromatic filled contours) hard X-ray selected AGN from Oh et al. (2017) and high- z X-ray selected broad-line AGN ($\langle z \rangle \sim 1.327$, color-filled stars). The dotted lines represent the loci of Eddington ratios.

to -0.1 . On the other hand, samples used in Oh et al. (2017) and this work are X-ray selected AGN in a lower redshift ($\langle z \rangle = 0.036$ and 1.327 , respectively) representing the majority of AGN populations with wide ranges of L_{bol} (~ 3.5 dex), M_{BH} (~ 4 dex), and λ_{Edd} (~ 4 dex). Therefore, we interpret the anti-correlated observational relation in $[\text{N II}]\lambda 6583/\text{H}\alpha$ vs. λ_{Edd} as a global feature appearing in narrow-line region of typical AGN at $z < 1.7$.

In this work, we do not find evidence of metallicity evolution of AGN with the redshift. The $[\text{N II}]\lambda 6583/\text{H}\alpha$ ratio, which is often used as a metallicity indicator, and its distribution of local and high- z AGN shown in Fig. 2 appear similar trend in a limited range of $\log \lambda_{\text{Edd}}$ (at > -1.81) as mentioned in Section 3. This is consistent with previous studies, which presented that the gas-phase metallicity of AGN has been shown to be constant in super-solar across the majority of cosmic time unlike inactive galaxies (Dietrich et al. 2003; Nagao et al. 2006b; Juarez et al. 2009; Matsuoka et al. 2009; Dors et al. 2014).

5. SUMMARY

We have presented observational results on the relationship between AGN Eddington ratio (λ_{Edd}) and narrow emission line ratio ($[\text{N II}]\lambda 6583/\text{H}\alpha$) using 53 X-ray selected broad-line AGN at $0.6 < z < 1.7$ compiled from the literature and the spectroscopic observations. Our main findings are as follows.

- The distribution of $[\text{N II}]\lambda 6583/\text{H}\alpha$ for X-ray selected broad-line AGN at $0.6 < z < 1.7$ as a function of λ_{Edd} is similar with those of local AGN at $\langle z \rangle = 0.036$, providing an observational clue that $[\text{N II}]\lambda 6583/\text{H}\alpha$ vs. λ_{Edd} relation still holds well up to the given redshift. However, it is difficult to draw a statistically definite conclusion on the linear regression analysis, due to paucity of low λ_{Edd} sources in high- z regime.
- The observed trend between λ_{Edd} and $[\text{N II}]\lambda 6583/\text{H}\alpha$ ratio could be explained by considering the mass-metallicity relation, X-ray heating processes, and prevalent radiatively driven outflows that depend on the λ_{Edd} state.
- Metallicity evolution of AGN is not observed, which is consistent with the literatures.

Table 2. Properties of High-redshift Broad-Line AGN

Source ^a	Field ^b	ID ^c	z	$\log([\text{N II}]\lambda 6583/\text{H}\alpha)$	$\log L_{\text{bol}}^{\text{d}}$	$\log(M_{\text{BH}}/M_{\odot})$	$\log \lambda_{\text{Edd}}$
KM10	CCLS	543	1.300	-0.46	45.12	8.38	-1.37
KM10	CCLS	1930	1.565	-0.08	45.87	8.61	-0.86
KM13	CCLS	142	0.699	-0.06	45.41	8.04	-0.75
KM13	CCLS	192	1.222	-0.18	45.44	7.68	-0.35
KM13	CCLS	208	1.242	-0.11	46.19	9.10	-1.02
KM13	CCLS	607	1.297	-0.22	45.99	8.21	-0.33
KM13	CCLS	1194	1.314	-0.16	44.87	7.56	-0.80
KM13	CCLS	549	1.319	-0.19	46.59	8.99	-0.51
KM13	CCLS	112	1.322	-0.08	46.06	8.62	-0.68
KM13	CCLS	463	1.327	0.08	45.42	7.37	-0.07
KM13	CCLS	157	1.332	-0.10	45.46	8.28	-0.94
KM13	CCLS	604	1.345	-0.41	45.57	7.57	-0.12
KM13	CCLS	546	1.407	-0.00	45.90	8.69	-0.90
KM13	CCLS	499	1.454	-0.11	46.25	8.70	-0.57
KM13	CCLS	119	1.505	-0.17	45.48	8.05	-0.69
KM13	CCLS	1044	1.561	0.19	46.10	8.50	-0.52
KM13	CCLS	216	1.567	-0.09	45.23	7.65	-0.54
KM13	CCLS	305	1.572	-0.32	45.73	8.62	-1.00
KM13	CCLS	255	1.667	-0.32	45.64	8.15	-0.62
N12	SXDS	328	0.809	-0.15	44.81	8.20	-1.50
N12	SXDS	353	0.989	-0.52	44.65	7.40	-0.86
N12	SXDS	332	1.385	-0.64	45.63	8.30	-0.78
N12	SXDS	763	1.413	-0.19	45.75	8.00	-0.36
N12	SXDS	735	1.447	-0.01	45.36	8.40	-1.15
N12	SXDS	18	1.452	-0.12	45.72	8.90	-1.29
N12	SXDS	1216	1.472	-0.28	45.85	9.30	-1.56
N12	SXDS	969	1.585	-0.32	45.13	8.20	-1.18
N12	SXDS	632	1.593	-0.06	45.72	9.10	-1.49
S15	CDFS	716	0.763	-0.37	44.93	7.98	-1.16
S15	LH	456	0.877	-0.52	45.28	7.53	-0.36
S15	CDFS	329	0.954	-0.15	44.26	6.97	-0.82
S15	LH	475	1.205	-0.49	47.07	9.08	-0.12
S15	CDFS	417	1.222	-0.26	45.33	9.03	-1.81
S15	LH	406	1.283	-0.17	45.39	8.87	-1.59
S15	LH	119	1.406	-0.17	45.25	8.47	-1.33
S15	LH	553	1.440	-0.54	46.36	8.75	-0.50
S15	LH	25	1.599	-0.18	44.52	7.15	-0.74
S15	CDFS	89	1.613	-0.24	44.44	7.54	-1.21
S15	CDFS	358	1.626	-0.44	45.64	8.28	-0.75
H16	SXDS	194	0.627	-0.94	44.48	7.52	-1.15
H16	SXDS	827	0.658	-0.30	44.62	7.49	-0.99
H16	CDFS	629	0.667	0.08	43.96	8.13	-2.29
H16	SXDS	393	0.822	-0.28	44.73	7.95	-1.34
H16	SXDS	600	0.873	-0.26	44.46	7.07	-0.73
H16	SXDS	883	0.961	0.26	45.67	8.23	-0.67
H16	CDFS	101	0.977	-0.02	45.25	8.51	-1.37
S19	CCLS	110	0.729	-0.42	44.92	7.70	-0.89
S19	CCLS	381	0.767	-0.74	45.16	7.57	-0.52
S19	CCLS	644	0.986	-0.19	45.18	8.10	-1.03
S19	CCLS	454	1.485	0.07	45.32	8.24	-1.04
S19	CCLS	512	1.516	0.03	45.64	8.13	-0.60
S19	CCLS	1590	1.596	-0.26	45.65	8.71	-1.17
S19	CCLS	1273	1.622	-0.37	45.18	8.46	-1.39

^a Source of literature: KM10 (Kartaltepe et al. 2015; Merloni et al. 2010); KM13 (Kartaltepe et al. 2015; Matsuoka et al. 2013); N12 (Nobuta et al. 2012); S15 (Suh et al. 2015); H16 (Harrison et al. 2016); S19 (Suh et al. in prep.).

^b Field name that used to measure 2 – 10 keV luminosity: CCLS (Civano et al. 2016); SXDS (Ueda et al. 2008); CDFS (Xue et al. 2011); LH (Brunner et al. 2008).

^c X-ray source ID from the literature.

^d In units of erg s^{-1} .

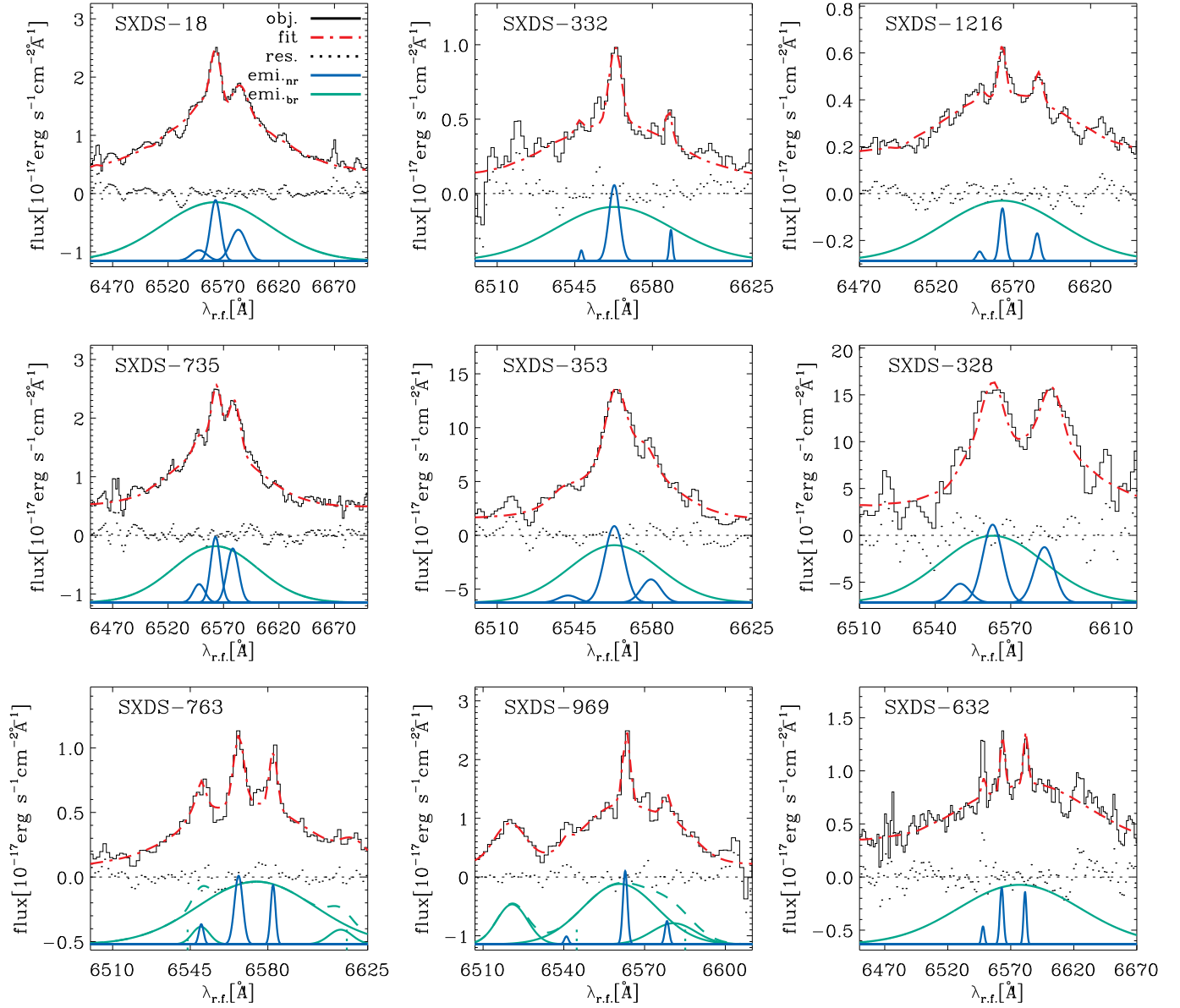


Figure 5. spectral line fit for 9 sources from [Nobuta et al. \(2012\)](#). Black lines present the observed spectra. Blue and green Gaussians indicate narrow and broad emission-line components, respectively. Red dash-dot line is the combined fit. Residuals are shown with black dots.

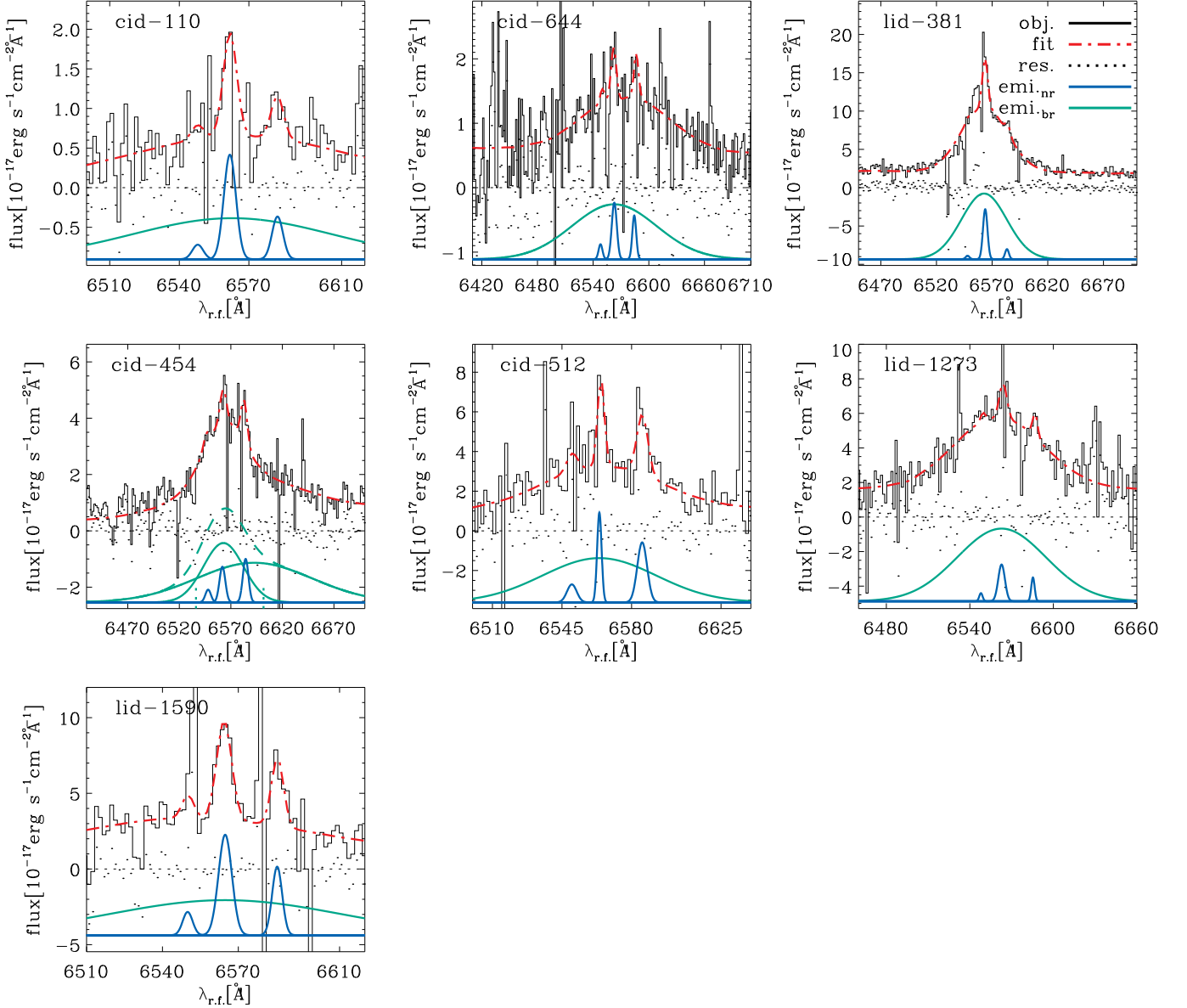


Figure 6. Spectral line fit for 7 sources from Suh et al. (*in prep.*). The format is the same as that of Fig. 5.

We thank Richard Mushotzky for taking the time to give valuable advice. K.O. acknowledges support from the Japan Society for the Promotion of Science (JSPS, ID: 17321). Part of this work was financially supported by the Grant-in-Aid for Scientific Research 17K05384 (Y.U.). M.K. acknowledges support from NASA through ADAP award NNH16CT03C.

This research has made use of NASA’s ADS Service. This research has made use of the NASA/ IPAC Infrared

Science Archive, which is operated by the Jet Propulsion Laboratory, California Institute of Technology, under contract with the National Aeronautics and Space Administration.

Facilities: Subaru(FMOS), IRSA

Software: gandalf (Sarzi et al. 2006)

REFERENCES

- Abazajian, K. N., Adelman-McCarthy, J. K., Agüeros, M. A., et al. 2009, *ApJS*, 182, 543, doi: [10.1088/0067-0049/182/2/543](https://doi.org/10.1088/0067-0049/182/2/543)
- Akiyama, M., Ueda, Y., Watson, M. G., et al. 2015, *PASJ*, 67, 82, doi: [10.1093/pasj/psv050](https://doi.org/10.1093/pasj/psv050)

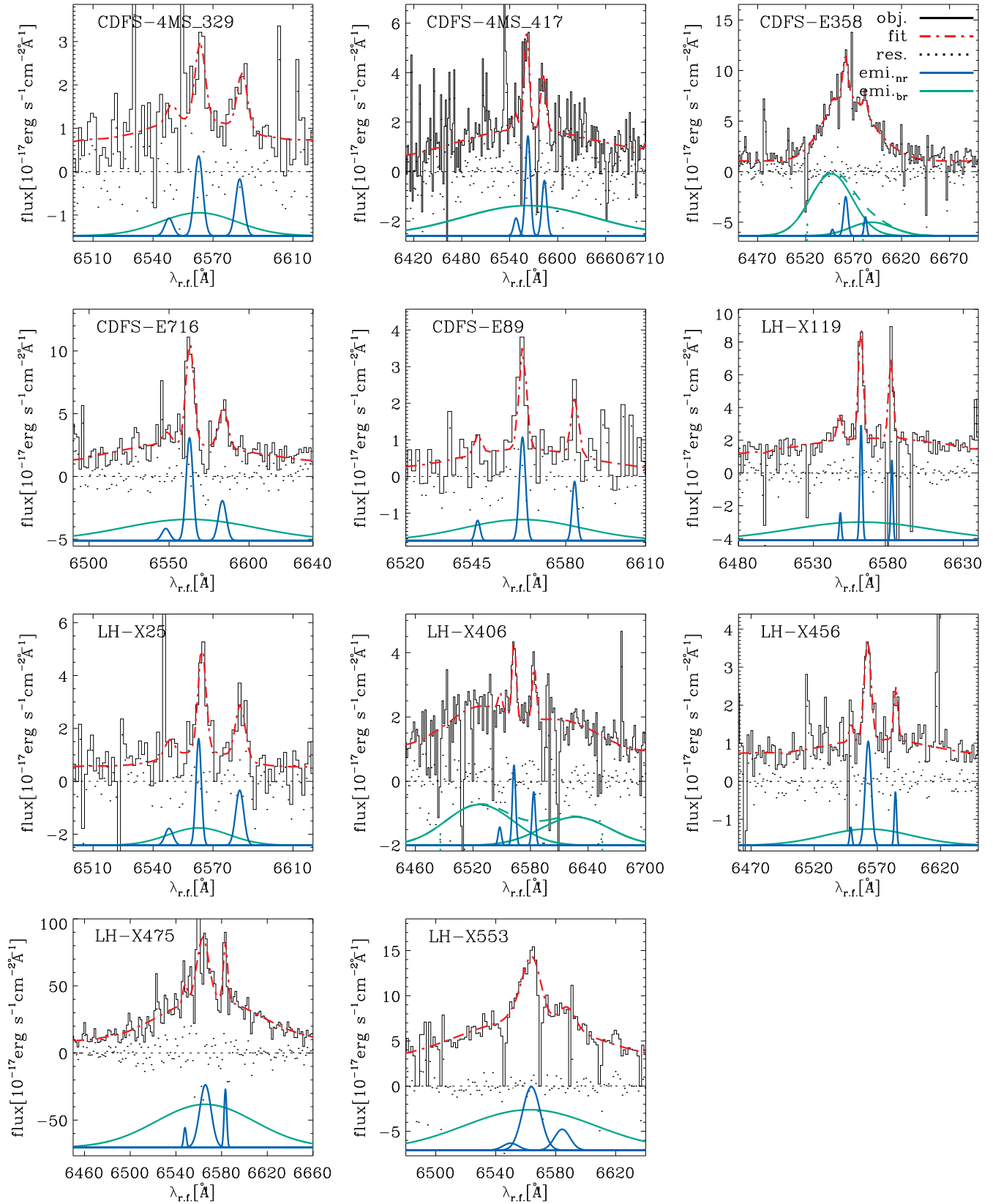


Figure 7. Spectral line fit for 11 sources from Suh et al. (2015). The format is the same as that of Fig. 5.

- Alam, S., Albareti, F. D., Allende Prieto, C., et al. 2015, *ApJS*, 219, 12, doi: [10.1088/0067-0049/219/1/12](https://doi.org/10.1088/0067-0049/219/1/12)
- Antonucci, R. 1993, *ARA&A*, 31, 473, doi: [10.1146/annurev.aa.31.090193.002353](https://doi.org/10.1146/annurev.aa.31.090193.002353)
- Bacon, R., Copin, Y., Monnet, G., et al. 2001, *MNRAS*, 326, 23, doi: [10.1046/j.1365-8711.2001.04612.x](https://doi.org/10.1046/j.1365-8711.2001.04612.x)
- Baldwin, J. A., Phillips, M. M., & Terlevich, R. 1981, *PASP*, 93, 5, doi: [10.1086/130766](https://doi.org/10.1086/130766)
- Barger, A. J., Cowie, L. L., Mushotzky, R. F., & Richards, E. A. 2001, *AJ*, 121, 662, doi: [10.1086/318742](https://doi.org/10.1086/318742)
- Barthelmy, S. D., Barbier, L. M., Cummings, J. R., et al. 2005, *SSRv*, 120, 143, doi: [10.1007/s11214-005-5096-3](https://doi.org/10.1007/s11214-005-5096-3)
- Baumgartner, W. H., Tueller, J., Markwardt, C. B., et al. 2013, *ApJS*, 207, 19, doi: [10.1088/0067-0049/207/2/19](https://doi.org/10.1088/0067-0049/207/2/19)
- Bentz, M. C., Peterson, B. M., Pogge, R. W., Vestergaard, M., & Onken, C. A. 2006, *ApJ*, 644, 133, doi: [10.1086/503537](https://doi.org/10.1086/503537)
- Bentz, M. C., Denney, K. D., Grier, C. J., et al. 2013, *ApJ*, 767, 149, doi: [10.1088/0004-637X/767/2/149](https://doi.org/10.1088/0004-637X/767/2/149)
- Brandt, W. N., & Alexander, D. M. 2010, *Proceedings of the National Academy of Science*, 107, 7184, doi: [10.1073/pnas.0914151107](https://doi.org/10.1073/pnas.0914151107)
- Brunner, H., Cappelluti, N., Hasinger, G., et al. 2008, *A&A*, 479, 283, doi: [10.1051/0004-6361:20077687](https://doi.org/10.1051/0004-6361/20077687)
- Caccianiga, A., Severgnini, P., Della Ceca, R., et al. 2007, *A&A*, 470, 557, doi: [10.1051/0004-6361:20077732](https://doi.org/10.1051/0004-6361:20077732)
- Civano, F., Marchesi, S., Comastri, A., et al. 2016, *ApJ*, 819, 62, doi: [10.3847/0004-637X/819/1/62](https://doi.org/10.3847/0004-637X/819/1/62)
- Collin, S., Kawaguchi, T., Peterson, B. M., & Vestergaard, M. 2006, *A&A*, 456, 75, doi: [10.1051/0004-6361:20064878](https://doi.org/10.1051/0004-6361:20064878)
- Comastri, A., Mignoli, M., Ciliegi, P., et al. 2002, *ApJ*, 571, 771, doi: [10.1086/340016](https://doi.org/10.1086/340016)
- Dietrich, M., Hamann, F., Shields, J. C., et al. 2003, *ApJ*, 589, 722, doi: [10.1086/374662](https://doi.org/10.1086/374662)
- Dors, O. L., Cardaci, M. V., Hägele, G. F., & Krabbe, Å. C. 2014, *MNRAS*, 443, 1291, doi: [10.1093/mnras/stu1218](https://doi.org/10.1093/mnras/stu1218)
- Elvis, M., Schreier, E. J., Tonry, J., Davis, M., & Huchra, J. P. 1981, *ApJ*, 246, 20, doi: [10.1086/158894](https://doi.org/10.1086/158894)
- Garnett, D. R. 2002, *ApJ*, 581, 1019, doi: [10.1086/344301](https://doi.org/10.1086/344301)
- Gavignaud, I., Wisotzki, L., Bongiorno, A., et al. 2008, *A&A*, 492, 637, doi: [10.1051/0004-6361:20078957](https://doi.org/10.1051/0004-6361:20078957)
- Gehrels, N., Chincarini, G., Giommi, P., et al. 2004, *ApJ*, 611, 1005, doi: [10.1086/422091](https://doi.org/10.1086/422091)
- Greene, J. E., & Ho, L. C. 2005, *ApJ*, 630, 122, doi: [10.1086/431897](https://doi.org/10.1086/431897)
- Griffiths, R. E., Georgantopoulos, I., Boyle, B. J., et al. 1995, *MNRAS*, 275, 77, doi: [10.1093/mnras/275.1.77](https://doi.org/10.1093/mnras/275.1.77)
- Groves, B. A., Heckman, T. M., & Kauffmann, G. 2006, *MNRAS*, 371, 1559, doi: [10.1111/j.1365-2966.2006.10812.x](https://doi.org/10.1111/j.1365-2966.2006.10812.x)
- Hamann, F., & Ferland, G. 1999, *ARA&A*, 37, 487, doi: [10.1146/annurev.astro.37.1.487](https://doi.org/10.1146/annurev.astro.37.1.487)
- Harrison, C. M., Alexander, D. M., Mullaney, J. R., et al. 2016, *MNRAS*, 456, 1195, doi: [10.1093/mnras/stv2727](https://doi.org/10.1093/mnras/stv2727)
- Harrison, F. A., Craig, W. W., Christensen, F. E., et al. 2013, *ApJ*, 770, 103, doi: [10.1088/0004-637X/770/2/103](https://doi.org/10.1088/0004-637X/770/2/103)
- Hasinger, G., Capak, P., Salvato, M., et al. 2018, *ApJ*, 858, 77, doi: [10.3847/1538-4357/aabacf](https://doi.org/10.3847/1538-4357/aabacf)
- Iwasawa, K., Koyama, K., Awaki, H., et al. 1993, *ApJ*, 409, 155, doi: [10.1086/172651](https://doi.org/10.1086/172651)
- Jones, D. H., Read, M. A., Saunders, W., et al. 2009, *MNRAS*, 399, 683, doi: [10.1111/j.1365-2966.2009.15338.x](https://doi.org/10.1111/j.1365-2966.2009.15338.x)
- Juarez, Y., Maiolino, R., Mujica, R., et al. 2009, *A&A*, 494, L25, doi: [10.1051/0004-6361:200811415](https://doi.org/10.1051/0004-6361:200811415)
- Kartaltepe, J. S., Sanders, D. B., Silverman, J. D., et al. 2015, *ApJL*, 806, L35, doi: [10.1088/2041-8205/806/2/L35](https://doi.org/10.1088/2041-8205/806/2/L35)
- Kashino, D., Silverman, J. D., Sanders, D., et al. 2019, *ApJS*, 241, 10, doi: [10.3847/1538-4365/ab06c4](https://doi.org/10.3847/1538-4365/ab06c4)
- Kaspi, S., Maoz, D., Netzer, H., et al. 2005, *ApJ*, 629, 61, doi: [10.1086/431275](https://doi.org/10.1086/431275)
- Kaspi, S., Smith, P. S., Netzer, H., et al. 2000, *ApJ*, 533, 631, doi: [10.1086/308704](https://doi.org/10.1086/308704)
- Kewley, L. J., Dopita, M. A., Sutherland, R. S., Heisler, C. A., & Trevena, J. 2001, *ApJ*, 556, 121, doi: [10.1086/321545](https://doi.org/10.1086/321545)
- Kewley, L. J., Groves, B., Kauffmann, G., & Heckman, T. 2006, *MNRAS*, 372, 961, doi: [10.1111/j.1365-2966.2006.10859.x](https://doi.org/10.1111/j.1365-2966.2006.10859.x)
- Kimura, M., Maihara, T., Iwamuro, F., et al. 2010, *PASJ*, 62, 1135, doi: [10.1093/pasj/62.5.1135](https://doi.org/10.1093/pasj/62.5.1135)
- Koss, M., Trakhtenbrot, B., Ricci, C., et al. 2017, *ApJ*, 850, 74, doi: [10.3847/1538-4357/aa8ec9](https://doi.org/10.3847/1538-4357/aa8ec9)
- Koss, M. J., Assef, R., Baloković, M., et al. 2016, *ApJ*, 825, 85, doi: [10.3847/0004-637X/825/2/85](https://doi.org/10.3847/0004-637X/825/2/85)
- La Mura, G., Popović, L. Č., Ciroi, S., Rafanelli, P., & Ilić, D. 2007, *ApJ*, 671, 104, doi: [10.1086/522821](https://doi.org/10.1086/522821)
- Lamperti, I., Koss, M., Trakhtenbrot, B., et al. 2017, *MNRAS*, 467, 540, doi: [10.1093/mnras/stx055](https://doi.org/10.1093/mnras/stx055)
- Larson, R. B. 1974, *MNRAS*, 169, 229, doi: [10.1093/mnras/169.2.229](https://doi.org/10.1093/mnras/169.2.229)
- Lehmer, B. D., Brandt, W. N., Alexander, D. M., et al. 2005, *ApJS*, 161, 21, doi: [10.1086/444590](https://doi.org/10.1086/444590)
- Lusso, E., Comastri, A., Simmons, B. D., et al. 2012, *MNRAS*, 425, 623, doi: [10.1111/j.1365-2966.2012.21513.x](https://doi.org/10.1111/j.1365-2966.2012.21513.x)
- Malkan, M. A., Jensen, L. D., Rodriguez, D. R., Spinoglio, L., & Rush, B. 2017, *ApJ*, 846, 102, doi: [10.3847/1538-4357/aa8302](https://doi.org/10.3847/1538-4357/aa8302)
- Marchesi, S., Ajello, M., Marcotulli, L., et al. 2018, *ApJ*, 854, 49, doi: [10.3847/1538-4357/aaa410](https://doi.org/10.3847/1538-4357/aaa410)

- Markwardt, C. B., Tueller, J., Skinner, G. K., et al. 2005, *ApJL*, 633, L77, doi: [10.1086/498569](https://doi.org/10.1086/498569)
- Matsuoka, K., Nagao, T., Maiolino, R., Marconi, A., & Taniguchi, Y. 2009, *A&A*, 503, 721, doi: [10.1051/0004-6361/200811478](https://doi.org/10.1051/0004-6361/200811478)
- Matsuoka, K., Nagao, T., Marconi, A., Maiolino, R., & Taniguchi, Y. 2011, *A&A*, 527, A100, doi: [10.1051/0004-6361/201015584](https://doi.org/10.1051/0004-6361/201015584)
- Matsuoka, K., Silverman, J. D., Schramm, M., et al. 2013, *ApJ*, 771, 64, doi: [10.1088/0004-637X/771/1/64](https://doi.org/10.1088/0004-637X/771/1/64)
- McGill, K. L., Woo, J.-H., Treu, T., & Malkan, M. A. 2008, *ApJ*, 673, 703, doi: [10.1086/524349](https://doi.org/10.1086/524349)
- McLure, R. J., & Dunlop, J. S. 2002, *MNRAS*, 331, 795, doi: [10.1046/j.1365-8711.2002.05236.x](https://doi.org/10.1046/j.1365-8711.2002.05236.x)
- Merloni, A., Bongiorno, A., Bolzonella, M., et al. 2010, *ApJ*, 708, 137, doi: [10.1088/0004-637X/708/1/137](https://doi.org/10.1088/0004-637X/708/1/137)
- Mullaney, J. R., & Ward, M. J. 2008, *MNRAS*, 385, 53, doi: [10.1111/j.1365-2966.2007.12777.x](https://doi.org/10.1111/j.1365-2966.2007.12777.x)
- Nagao, T., Maiolino, R., & Marconi, A. 2006a, *A&A*, 447, 863, doi: [10.1051/0004-6361:20054127](https://doi.org/10.1051/0004-6361:20054127)
- Nagao, T., Marconi, A., & Maiolino, R. 2006b, *A&A*, 447, 157, doi: [10.1051/0004-6361:20054024](https://doi.org/10.1051/0004-6361:20054024)
- Netzer, H., & Trakhtenbrot, B. 2007, *ApJ*, 654, 754, doi: [10.1086/509650](https://doi.org/10.1086/509650)
- Nobuta, K., Akiyama, M., Ueda, Y., et al. 2012, *ApJ*, 761, 143, doi: [10.1088/0004-637X/761/2/143](https://doi.org/10.1088/0004-637X/761/2/143)
- Oh, K., Sarzi, M., Schawinski, K., & Yi, S. K. 2011, *ApJS*, 195, 13, doi: [10.1088/0067-0049/195/2/13](https://doi.org/10.1088/0067-0049/195/2/13)
- Oh, K., Yi, S. K., Schawinski, K., et al. 2015, *ApJS*, 219, 1, doi: [10.1088/0067-0049/219/1/1](https://doi.org/10.1088/0067-0049/219/1/1)
- Oh, K., Schawinski, K., Koss, M., et al. 2017, *MNRAS*, 464, 1466, doi: [10.1093/mnras/stw2467](https://doi.org/10.1093/mnras/stw2467)
- Oh, K., Koss, M., Markwardt, C. B., et al. 2018, *ApJS*, 235, 4, doi: [10.3847/1538-4365/aaa7fd](https://doi.org/10.3847/1538-4365/aaa7fd)
- Ricci, C., Ueda, Y., Koss, M. J., et al. 2015, *ApJL*, 815, L13, doi: [10.1088/2041-8205/815/1/L13](https://doi.org/10.1088/2041-8205/815/1/L13)
- Ricci, C., Trakhtenbrot, B., Koss, M. J., et al. 2017, *ApJS*, 233, 17, doi: [10.3847/1538-4365/aa96ad](https://doi.org/10.3847/1538-4365/aa96ad)
- Rigby, J. R., Rieke, G. H., Donley, J. L., Alonso-Herrero, A., & Pérez-González, P. G. 2006, *ApJ*, 645, 115, doi: [10.1086/504067](https://doi.org/10.1086/504067)
- Sarzi, M., Falcón-Barroso, J., Davies, R. L., et al. 2006, *MNRAS*, 366, 1151, doi: [10.1111/j.1365-2966.2005.09839.x](https://doi.org/10.1111/j.1365-2966.2005.09839.x)
- Schawinski, K., Thomas, D., Sarzi, M., et al. 2007, *MNRAS*, 382, 1415, doi: [10.1111/j.1365-2966.2007.12487.x](https://doi.org/10.1111/j.1365-2966.2007.12487.x)
- Schlafly, E. F., & Finkbeiner, D. P. 2011, *ApJ*, 737, 103, doi: [10.1088/0004-637X/737/2/103](https://doi.org/10.1088/0004-637X/737/2/103)
- Schulze, A., Silverman, J. D., Kashino, D., et al. 2018, *ApJS*, 239, 22, doi: [10.3847/1538-4365/aae82f](https://doi.org/10.3847/1538-4365/aae82f)
- Sekiguchi, K., Akiyama, M., Furusawa, H., et al. 2005, in *Multiwavelength Mapping of Galaxy Formation and Evolution*, ed. A. Renzini & R. Bender, Vol. 2005925391, 82
- Shemmer, O., & Netzer, H. 2002, *ApJL*, 567, L19, doi: [10.1086/339797](https://doi.org/10.1086/339797)
- Shen, Y., Greene, J. E., Strauss, M. A., Richards, G. T., & Schneider, D. P. 2008, *ApJ*, 680, 169, doi: [10.1086/587475](https://doi.org/10.1086/587475)
- Shen, Y., & Liu, X. 2012, *ApJ*, 753, 125, doi: [10.1088/0004-637X/753/2/125](https://doi.org/10.1088/0004-637X/753/2/125)
- Shen, Y., Richards, G. T., Strauss, M. A., et al. 2011, *ApJS*, 194, 45, doi: [10.1088/0067-0049/194/2/45](https://doi.org/10.1088/0067-0049/194/2/45)
- Silverman, J. D., Kashino, D., Sanders, D., et al. 2015, *ApJS*, 220, 12, doi: [10.1088/0067-0049/220/1/12](https://doi.org/10.1088/0067-0049/220/1/12)
- Stern, J., & Laor, A. 2013, *MNRAS*, 431, 836, doi: [10.1093/mnras/stt211](https://doi.org/10.1093/mnras/stt211)
- Suh, H., Hasinger, G., Steinhardt, C., Silverman, J. D., & Schramm, M. 2015, *ApJ*, 815, 129, doi: [10.1088/0004-637X/815/2/129](https://doi.org/10.1088/0004-637X/815/2/129)
- Trakhtenbrot, B., & Netzer, H. 2012, *MNRAS*, 427, 3081, doi: [10.1111/j.1365-2966.2012.22056.x](https://doi.org/10.1111/j.1365-2966.2012.22056.x)
- Tremonti, C. A., Heckman, T. M., Kauffmann, G., et al. 2004, *ApJ*, 613, 898, doi: [10.1086/423264](https://doi.org/10.1086/423264)
- Trump, J. R., Sun, M., Zeimann, G. R., et al. 2015, *ApJ*, 811, 26, doi: [10.1088/0004-637X/811/1/26](https://doi.org/10.1088/0004-637X/811/1/26)
- Tueller, J., Mushotzky, R. F., Barthelmy, S., et al. 2008, *ApJ*, 681, 113, doi: [10.1086/588458](https://doi.org/10.1086/588458)
- Tueller, J., Baumgartner, W. H., Markwardt, C. B., et al. 2010, *ApJS*, 186, 378, doi: [10.1088/0067-0049/186/2/378](https://doi.org/10.1088/0067-0049/186/2/378)
- Ueda, Y., Watson, M. G., Stewart, I. M., et al. 2008, *ApJS*, 179, 124, doi: [10.1086/591083](https://doi.org/10.1086/591083)
- Urry, C. M., & Padovani, P. 1995, *PASP*, 107, 803, doi: [10.1086/133630](https://doi.org/10.1086/133630)
- Vasudevan, R. V., Mushotzky, R. F., Winter, L. M., & Fabian, A. C. 2009, *MNRAS*, 399, 1553, doi: [10.1111/j.1365-2966.2009.15371.x](https://doi.org/10.1111/j.1365-2966.2009.15371.x)
- Veilleux, S., & Osterbrock, D. E. 1987, *ApJS*, 63, 295, doi: [10.1086/191166](https://doi.org/10.1086/191166)
- Vestergaard, M. 2002, *ApJ*, 571, 733, doi: [10.1086/340045](https://doi.org/10.1086/340045)
- Vestergaard, M., & Osmer, P. S. 2009, *ApJ*, 699, 800, doi: [10.1088/0004-637X/699/1/800](https://doi.org/10.1088/0004-637X/699/1/800)
- Warner, C., Hamann, F., & Dietrich, M. 2004, *ApJ*, 608, 136, doi: [10.1086/386325](https://doi.org/10.1086/386325)
- Winkler, C., Courvoisier, T. J.-L., Di Cocco, G., et al. 2003, *A&A*, 411, L1, doi: [10.1051/0004-6361:20031288](https://doi.org/10.1051/0004-6361:20031288)
- Woo, J.-H., & Urry, C. M. 2002, *ApJ*, 579, 530, doi: [10.1086/342878](https://doi.org/10.1086/342878)
- Xue, Y. Q., Luo, B., Brandt, W. N., et al. 2011, *ApJS*, 195, 10, doi: [10.1088/0067-0049/195/1/10](https://doi.org/10.1088/0067-0049/195/1/10)

York, D. G., Adelman, J., Anderson, Jr., J. E., et al. 2000,
AJ, 120, 1579, doi: [10.1086/301513](https://doi.org/10.1086/301513)